


 Cite this: *RSC Adv.*, 2025, 15, 50565

 Received 30th September 2025  
 Accepted 9th December 2025

DOI: 10.1039/d5ra07429k

[rsc.li/rsc-advances](https://rsc.li/rsc-advances)

# 7-Amino-2-(*N,N*-dimethylamino)quinazoline: a small, bright, easily synthesized scaffold for pH sensors

 Mohammed Mahdaly, Takeshi Maki, Ryuji Osako, Yuki Fujimaki and Yumiko Suzuki \*

This study reports a series of pH-responsive 2-(*N,N*-dimethylamino)quinazolines bearing amino substituents at position 7. These compounds exhibited tunable fluorescence (FL) enhancements under both acidic and basic conditions. Due to their small size, ease of synthesis, and strong fluorescence, these probes show promise for the development of pH sensors suitable for biological or environmental applications.

## 1 Introduction

Fluorophore-based pH sensors are molecular tools that exhibit fluorescence (FL) changes in response to pH variations. These sensors play a crucial role in biological research,<sup>1</sup> environmental monitoring,<sup>2</sup> and industrial applications,<sup>3</sup> where accurate pH detection is essential for understanding biochemical phenomena, optimizing reaction conditions, and ensuring product quality.<sup>4</sup> Effective pH sensor design requires fluorophores with  $pK_a$  values near the target pH range and functional groups that modulate FL through protonation or deprotonation.<sup>5</sup>

A wide range of synthetic fluorophores has been established for pH sensing applications, with representative molecular scaffolds including fluorescein,<sup>6</sup> rhodamine,<sup>7</sup> coumarin,<sup>8</sup> xanthenes,<sup>9</sup> BODIPY,<sup>10</sup> cyanine,<sup>11</sup> pyranine,<sup>12</sup> and acridine.<sup>13</sup> These fluorophores have been successfully employed in various pH-responsive systems. However, many of these structures involve relatively large molecular frameworks and complex synthetic routes, which can lead to increased cytotoxicity and limited cell permeability, thereby compromising their biocompatibility.

In addition to the structural limitations, operational constraints further restrict the conventional probes' applicability. Fluorescein-based probes typically demonstrate a narrow pH sensitivity range, which limits their applicability across diverse experimental conditions,<sup>14,15</sup> while rhodamine-based probes function predominantly under acidic conditions due to the pH-dependent spiro-lactam ring-opening mechanism, thereby limiting their use in neutral or alkaline environments.<sup>16,17</sup> Recent efforts to develop alternative systems include a luminescent metal-organic framework probe (JXUST-29) that

exhibits pH-dependent emission with selectivity toward basic amino acids,<sup>18</sup> as well as a coumarin-based turn-on probe (DIC) that responds in the alkaline region.<sup>19</sup> However, these systems also operate effectively only within limited pH ranges, highlighting the need for compact fluorophores with broader pH responsiveness.

Small-molecule fluorophores based on quinazoline scaffolds have attracted considerable attention due to their compact structure and favourable photophysical characteristics.<sup>20–22</sup> Furthermore, quinazoline-based fluorescent probes exhibit several advantages for pH sensing applications, demonstrating broad and tunable pH sensitivity ranges,<sup>23,24</sup> excellent reversibility,<sup>25</sup> and favourable biocompatibility,<sup>26,27</sup> rendering them particularly suitable for biological,<sup>26–28</sup> environmental<sup>29</sup> and analytical investigations.<sup>30</sup> Their pH-responsive behaviour is often governed by photoinduced electron transfer (PET) or intramolecular charge transfer (ICT).

In a previous study on the development of 2-aminoquinazolines exhibiting distinct photophysical properties, these compounds were utilized for the development of  $\alpha$ -tubulin colchicine site competition assay and for visualizing the intracellular distribution of the fluorophore by FL microscopy.<sup>31</sup> In addition, the compound 7-amino-4-methoxyl-2-*N*-morpholinoquinazoline was reported, which exhibited enhanced FL under acidic conditions.<sup>32</sup> Notably, (di-(2-picolyl)amino)quinazoline derivatives have also been applied to ATP sensing *via* a copper-mediated fluorescence on-off system.<sup>33</sup> Despite these promising features, the exploration of quinazoline derivatives as pH-responsive probes with a broad pH range remains limited.

This study presents a new class of easily synthesized 7-amino-2-(*N,N*-dimethylamino)quinazoline derivatives as pH-sensitive fluorophores. The investigation focused on their photoluminescence behavior and solvatochromic properties across various solvents, including water. These findings provide valuable insights into the design principles for small-molecule

Department of Materials and Life Sciences, Faculty of Science and Technology, Sophia University, 7-1 Kioi-cho, Chiyoda-ku, Tokyo 102-8554, Japan. E-mail: yumiko\_suzuki@sophia.ac.jp



pH sensors capable of detecting a wide range of pH values, with potential applications in chemical and biological systems.

## 2. Results and discussion

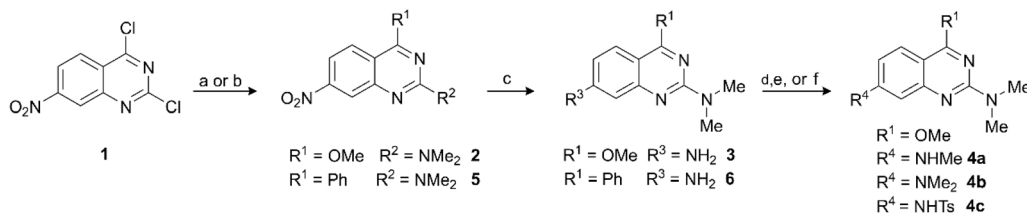
The synthesis of 7-amino-2-(*N,N*-dimethylamino)quinazoline derivatives was initiated from 2,4-dichloro-7-nitroquinazoline **1**, which underwent regioselective nucleophilic substitutions at positions 2 and 4 to afford compound **2** (Scheme 1). Subsequent reduction of the nitro group yielded the 7-amino derivative **3**. The 7-amino group of **3** was further functionalized *via* methylation, dimethylation, or tosylation, affording compounds **4a**, **4b**, or **4c**, respectively. In addition, a phenyl-substituted analogue **6** was successfully synthesized from **1** *via* a Suzuki–Miyaura cross-coupling reaction at position 4, followed by nucleophilic substitution at position 2 and reduction of the nitro group, highlighting the synthetic flexibility of the scaffold.

Photophysical properties, including UV-vis absorption and photoluminescence emission (PLE) spectra, of the synthesized compounds were systematically investigated (Table 1). Absolute FL quantum yields ( $\phi_F$ ) were determined in spectroscopic-grade DMSO ( $10^{-5}$  M) using an integrating sphere, demonstrating sufficient efficiency of the fluorophores. FL measurements in various spectroscopic-grade solvents ( $10^{-5}$  M, 1% DMSO) showed that the FL intensity varied across solvents with minimal spectral shifts. (Detailed spectral data are provided in the SI).

FL measurements under various pH conditions were performed in 1% DMSO solutions ( $10^{-5}$  M), with pH adjusted by controlled addition of HCl or NaOH, and excitation wavelengths set at isosbestic points identified in the UV-vis spectra. Additionally, the  $pK_a$  values were determined from the FL spectra of the probes across various pH levels (Table 1). For comparison, the FL-based pH-response of the previously reported 2-(*N,N*-dimethylamino)-4-methoxyquinazoline **7** was also examined.

Compound **3** (7-NH<sub>2</sub>) exhibited a prominent absorption band with a maximum ( $^{abs}\lambda_{max}$ ) at approximately 300 nm, which remained largely unaffected across the pH range (Fig. 1, see also Fig. 13S, SI). However, spectral variations were evident outside the 280–320 nm window. Changes in the short-wavelength region (<285 nm) may reflect modulations in  $n \rightarrow \pi^*$  transitions involving nitrogen lone pairs, while those in the long-wavelength region (>350 nm) could be attributed to subtle shifts in charge-transfer interactions influenced by protonation or deprotonation. A similar trend was observed for compound **7** without the amino group at position 7, with its stable absorption band centred around 302 nm and pH-dependent variations occurring primarily outside the 288–330 nm range (see Fig. 21S, SI).

Compound **3** exhibited intense FL at pH 2–7 ( $^{em}\lambda_{max} = 391.8$  nm) with a FL intensity approximately 4.5-fold higher than the intensity under basic conditions (pH 9–12), where the emission was red-shifted to 405.6 nm (Fig. 1). From the pH-dependent FL intensity profile, a  $pK_a$  value of 8.0 was obtained (Fig. 2 and



**Scheme 1** Synthesis of 7-amino-2-(*N,N*-dimethylamino)quinazoline derivatives. Reaction conditions: (a) for **2**: (i) NaOMe, MeOH, 0 °C, 2.5 h (ii) Me<sub>2</sub>NH, MeOH, rt, 20 h, 93%. (b) for **5**: (i) PhB(OH)<sub>2</sub>, Pd(PPh<sub>3</sub>)<sub>4</sub>, K<sub>2</sub>CO<sub>3</sub>, toluene, reflux, 3 h, 69%; (ii) Me<sub>2</sub>NH, 1,4-dioxane, reflux, 3 h, 91%. (c) for **3** and **6**: Pd/C 10 mol%, H<sub>2</sub> atm, MeOH, rt, 20 h, **3** (85%) and **6** (18%). (e) for **4a**: MeI, Cs<sub>2</sub>CO<sub>3</sub>, DMF, rt, 66 h, 22%. (f) for **4b**: HCHO, HCO<sub>2</sub>H, reflux, 5 h, 20%. (g) for **4c**: *p*-TsCl, pyridine, DCM, rt, 18 h, 98%.

**Table 1** Spectroscopic properties of 7-amino-2-(*N,N*-dimethylamino)quinazoline derivatives in DMSO and  $pK_a$  values in aqueous media (1% DMSO)

Compound	UV-vis $^{abs}\lambda_{max}$ nm <sup>a</sup>	PLE <sup>solution</sup> $^{em}\lambda_{max}$ , nm ( $\lambda_{ex}$ ) <sup>a</sup>	Stokes shift cm <sup>-1</sup>	$\phi_F$ solution [ $\lambda_{ex}$ , nm]	$pK_a$ H value <sup>b</sup>
<b>3</b>	246	400 (265 nm)	17 838	17 [330 nm]	8.0
	342		9199		
<b>4a</b>	258	424 (260 nm)	15 174	18 [330 nm]	8.1
	355		4584		
<b>4b</b>	256	411 (270 nm)	14 731	19 [330 nm]	8.1
	350		4240		
<b>4c</b>	260	420 (270 nm)	14 652	31 [330 nm]	7.4
	350		4761		
<b>6</b>	266	505 (280 nm)	17 792	7 [350 nm]	6.7
	366		7520		
<b>7</b>	282	430 (277 nm)	12 205	69 [330 nm]	7.0
	355		4913		

<sup>a</sup> Spectra were recorded at room temperature at  $c = 10^{-5}$  M in DMSO. <sup>b</sup> Calculated from FL spectra under various pH conditions.



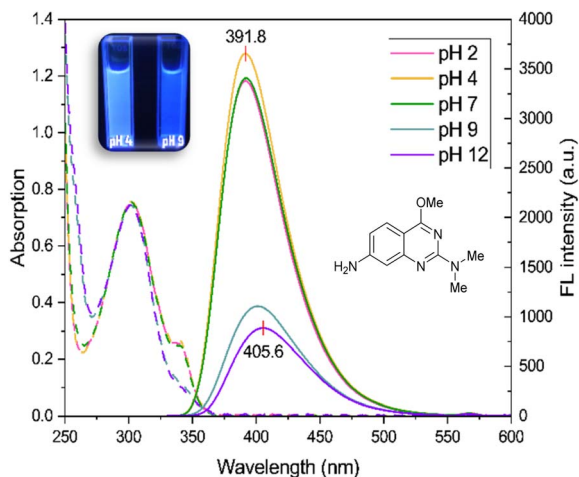


Fig. 1 UV-vis and fluorescence spectra at  $\lambda_{\text{ex}}$  285 nm of **3** under various pH conditions.

Table 1). The “turn-off” response under basic conditions is attributed to the  $\text{NH}_2$  group acting as an electron donor, which facilitates a PET process that quenches the FL. In contrast, compound **7**, which lacks the 7- $\text{NH}_2$  group, was fluorescent under neutral and basic conditions; however, its emission was quenched under acidic conditions (see Fig. 21S and 22S, SI). This suggests that protonation of compound **7** promotes non-radiative decay, highlighting the essential role of the 7-amino group.

To further investigate the protonation behavior,  $^1\text{H}$  NMR experiments were conducted using camphor sulfonic acid (Fig. 23S, SI). Upon acid addition, the methyl protons of the *N,N*-dimethylamino group of compound **3** exhibited downfield shifts (3.22 ppm to 3.6 ppm), splitting, and broadening, indicating electronic perturbation consistent with protonation at the N1 position (a similar trend was observed for compound **7**, supporting its protonation under acidic conditions; Fig. 24S, SI). Additionally, the  $\text{NH}_2$ -derived signal—likely representing an equilibrium between amino and imine forms (**I** and **II**, respectively, in Scheme 2)—also shifted downfield (4.00 ppm to 5.20 ppm) and broadened, along with the C8-H signal (6.64 ppm to 7.60 ppm). Under acidic conditions, the imine-type tautomer **II** may serve as the emissive species.

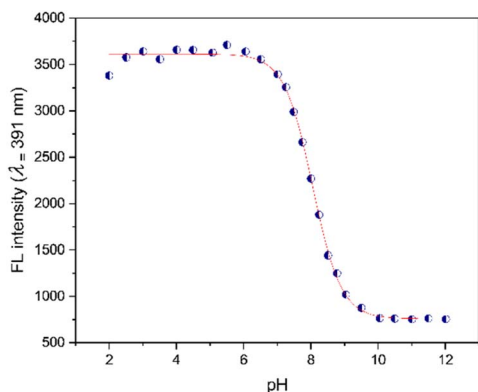
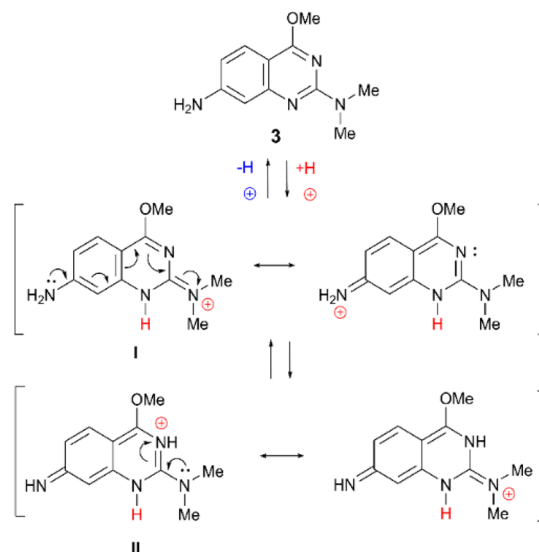


Fig. 2 pH-dependence of **3**  $\lambda_{\text{em}} = 391$  nm ( $\lambda_{\text{ex}} = 285$  nm),  $\text{p}K_{\text{a}}\text{H} = 8.0$ .



Scheme 2 Proposed mechanism of protonation and tautomerization under acidic condition of **3**.

To assess the reversibility of the FL response of compound **3**, pH cycling experiments were performed by alternating the pH between 4 and 9 for five cycles (Fig. 3). The FL intensity was recorded at each pH value at 1 hour intervals, and consistent emission levels were maintained at both pH 4 and pH 9 throughout the cycles. These results confirm the chemical and photophysical stability of the probes, enabling repeated pH monitoring without degradation.

Compound **6**, featuring a phenyl group at the 4-position of the quinazoline core instead of a methoxy group, displayed a photophysical profile similar to that of **3**, but with a significantly red-shifted emission (Fig. 4, see also Fig. 19S, SI). Under acidic conditions (pH 2–4), the FL maximum ( $^{\text{em}}\lambda_{\text{max}}$ ) was observed at 513 nm, representing a bathochromic shift of over 120 nm compared to **3**. This shift likely reflects partial stabilization of the excited state *via* extended  $\pi$ -conjugation, although the phenyl ring may not be fully coplanar with the quinazoline

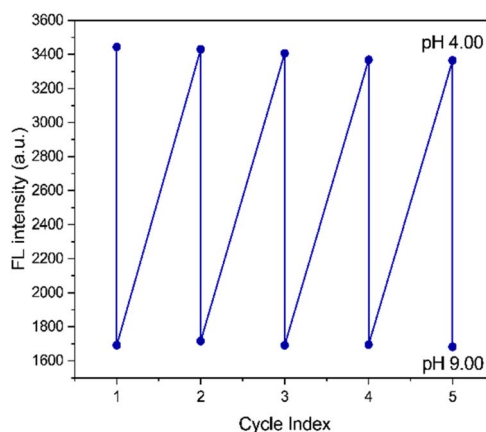


Fig. 3 Reversibility of **3** between pH 4.0 and pH 9.0 with 1 hour cycling intervals.



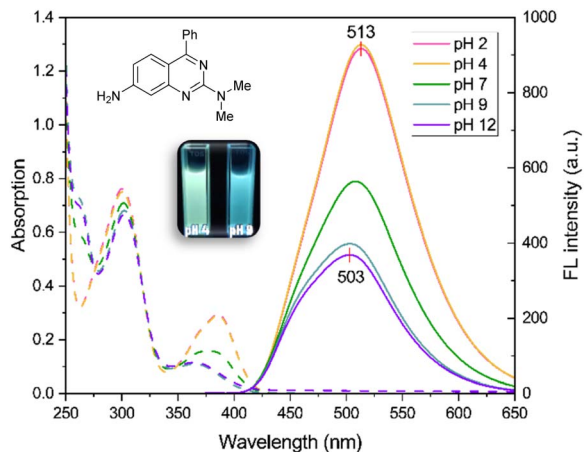


Fig. 4 UV-vis and fluorescence spectra at  $\lambda_{\text{ex}}$  277 nm of **6** under various pH conditions.

core. Similar to compound **3**, compound **6** showed pH-dependent FL behavior, exhibiting a 2.2-fold higher intensity under acidic conditions than under basic conditions (see Fig. 20S, SI). Its  $\text{pK}_{\text{aH}}$  value was 6.7 (Table 1), and the enhanced emission occurred with no significant change in the emission maximum.

Compound **4a** (7-NHMe) exhibited an absorption profile similar to that of **3**, with an absorption maximum at 300 nm (Fig. 5, see also Fig. 14S, SI). Under acidic to neutral pH, it showed strong FL with a slightly red-shifted emission maximum at 412 nm—approximately 20 nm bathochromic relative to **3**—likely due to stabilization of the excited state *via* (ICT) facilitated by the electron-donating methyl group. At pH 9–12, the FL was quenched without a significant shift in emission maximum, consistent with PET involving the lone pair electrons on the NHMe group. The probe exhibited a 2.8-fold increase in FL intensity under acidic conditions relative to basic conditions. The  $\text{pK}_{\text{aH}}$  was 8.1 (Table 1 and see also Fig. 15S, SI).

Compound **4c** (7-NHTs), bearing an electron-withdrawing tosyl group instead of an electron-donating methyl group,

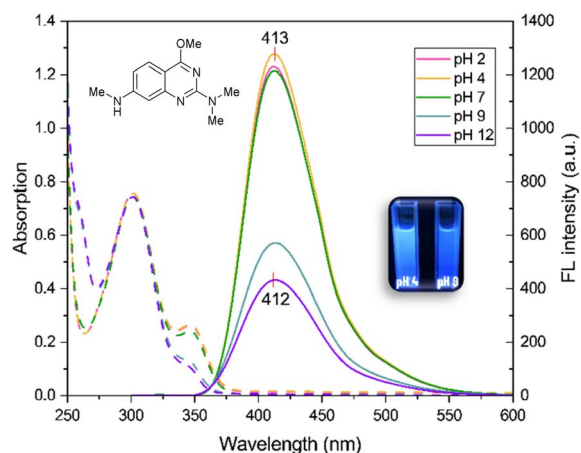


Fig. 5 UV-vis and fluorescence spectra at  $\lambda_{\text{ex}}$  290 nm of **4a** under various pH conditions.

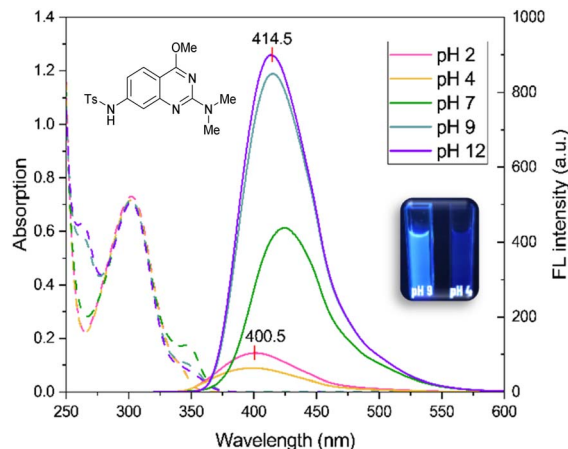


Fig. 6 UV-vis and fluorescence spectra at  $\lambda_{\text{ex}}$  283 nm of **4c** under various pH conditions.

displayed an absorption band similar to those of compounds **3** and **4a**. It exhibited “turn-on” FL under basic conditions, with an emission maximum ( $^{\text{em}}\lambda_{\text{max}}$ ) at 414.5 nm (Fig. 6, see also Fig. 18S, SI<sup>†</sup>). Under highly acidic conditions, it was almost non-fluorescent, whereas under basic conditions, the FL intensity increased by 11.2-fold (Fig. 7). Its  $\text{pK}_{\text{aH}}$  value was 7.4 (Table 1). The lone pair electrons on the nitrogen atom of the 7-NHTs group are likely delocalized toward the tosyl moiety, which may prevent the formation of a fluorescent imine-type tautomer **II** under acidic conditions, as observed in **3** and **4a**. Furthermore, this delocalization may suppress PET-based quenching under basic conditions.

Compound **4b** (7-NMe<sub>2</sub>), featuring dimethylation of the amino group at position 7, displayed the absorption band with a maximum at 300 nm, the intensity of which remained unchanged across the pH range from 2 to 12 (Fig. 8, see also Fig. 16S, SI). Its emission maximum was remarkably stable at 411 nm throughout this range. Unlike **3** and **4a**, its FL intensity increased monotonically with rising pH. Under basic conditions, the emission intensity was 3-fold higher than under

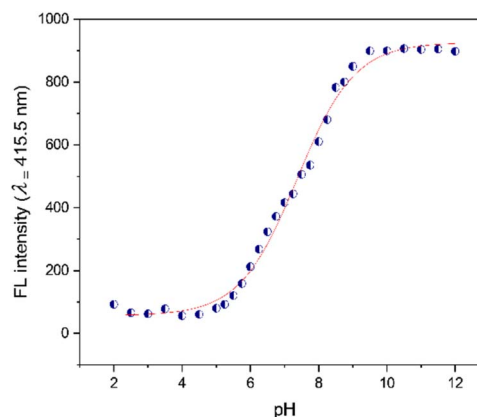


Fig. 7 pH-dependence of **4c**  $\lambda_{\text{em}} = 415.5$  nm ( $\lambda_{\text{ex}} = 283$  nm),  $\text{pK}_{\text{aH}} = 7.4$ .



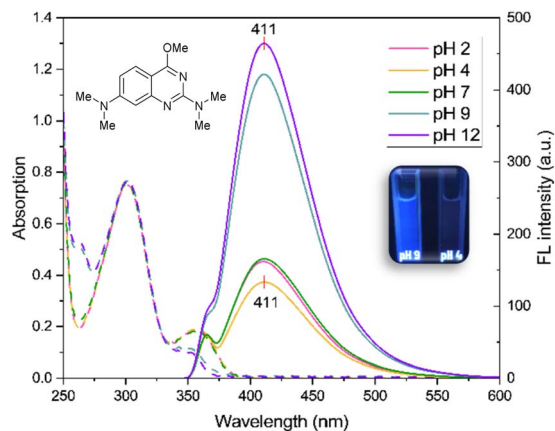


Fig. 8 UV-vis and fluorescence spectra at  $\lambda_{\text{ex}}$  325 nm of **4b** under various pH conditions.

acidic conditions (see Fig. 17S, SI). The probe showed a  $\text{p}K_{\text{aH}}$  of 8.1 (Table 1). This behavior reflects the absence of an N–H bond, which prevents the formation of the imine-type tautomer (**II** in compound **3**).

### 3 Conclusion

In summary, novel 7-amino-2-(*N,N*-dimethylamino)quinazoline derivatives were synthesized and characterized, demonstrating significant potential as fluorophore-based pH sensors. This study contributes to the development of quinazoline-based fluorophores for diverse sensing applications. The potential applications of these compounds extend beyond pH sensing and may include biological imaging, environmental monitoring, and chemical analysis. Further evaluation of selectivity and performance under simulated application conditions will be an important direction for future development. Building on these results, further efforts toward ratiometric pH sensors for biological systems are currently underway in our laboratory.

## 4 Experimental procedures of UV-vis and FL measurements

### 4.1 Preparation of solutions for measurements in various spectroscopic-grade solvents

The solutions for the measurement were prepared in 10  $\text{cm}^3$  volumetric flasks. All solutions were prepared with 1% DMSO – 99% solvent ( $\text{H}_2\text{O}$ , DMSO, MeCN, MeOH, 1,4-dioxane) (v/v), and the concentration of each quinazoline derivative was  $1.0 \times 10^{-5}$  M.

### 4.2 Preparation of solutions for pH profile

A  $1.0 \times 10^{-3}$  M stock solution of the compound was prepared by dissolving the compound in spectroscopic-grade DMSO in a 10  $\text{cm}^3$  volumetric flask. For the FL spectra measurements, 500  $\mu\text{L}$  of the stock solution was mixed with 5.0 mL HEPES/NaOH buffer, 5.0 mL  $\text{NaNO}_3$  solution, and water in a 50  $\text{cm}^3$  volumetric flask. The HEPES/NaOH buffer (50 mM, pH 7.42–7.45) was added to

maintain a buffer concentration of  $5.0 \times 10^{-3}$  M and prevent significant pH jumps. Ionic strength was controlled at 0.10 M using a 1 M  $\text{NaNO}_3$  aqueous solution. The pH of the solution was initially set to 2.0 by adding HCl aqueous solution, and NaOH and HCl aqueous solutions were used to adjust the pH while stirring with a magnetic stirrer. The total solution volume was adjusted to minimize concentration errors to within 3%.

### 4.3 General procedures of quantum yield $\phi_{\text{F}}$ measurement

The measurements and calculations were conducted using the ISF-834 integrating sphere unit attached to a JASCO Co. FP-8550 spectrofluorometer. DMSO served as the blank solvent, and the determination sample solutions ( $1.0 \times 10^{-5}$  M) in DMSO were recorded at room temperature.

### 4.4 General procedures of pH reversibility

The solution was prepared in the same manner as for the pH profile preparation. The pH reversibility was assessed at pH 4 and pH 9, repeated five times, and recorded at room temperature. Aqueous solutions of NaOH and HCl were used to adjust the pH and were stirred with a magnetic stirrer. The total solution volume was adjusted to minimize concentration errors to within 3%.

## Author contributions

Y. S. conceived and directed the project. M. M., T. M., R. O., and Y. F. performed experiments. Y. S. and M. M. wrote the manuscript.

## Conflicts of interest

There are no conflicts to declare.

## Data availability

Supplementary information (SI): experimental procedures, characterization data (NMR, mass spectrometry, UV-vis, and fluorescence spectra), and additional analytical results. See DOI: <https://doi.org/10.1039/d5ra07429k>.

## Acknowledgements

This work was supported by JSPS KAKENHI Grant Number JP15K07868, JP18K06587 and Sophia University. We thank Prof. Shinkoh Nanbu, Prof. Takeshi Hashimoto of the Faculty of Science and Technology, Sophia University, and Prof. Bernhard Witulski of Institut CARMEN (ex-LCMT) UMR CNRS 6507, ENSICAEN & UNICAEN, University of Normandy for useful discussions. We also thank Ms. Emiko Okano of the Faculty of Science and Technology, Sophia University, for the mass spectrometry measurements.



## Notes and references

- 1 R. Wang, C. Yu, F. Yu, L. Chen and C. Yu, *TrAC Trends Anal. Chem.*, 2010, **29**, 1004–1013.
- 2 M. Gao and B. Z. Tang, *ACS Sens.*, 2017, **2**, 1382–1399.
- 3 C. G. Frankær, K. J. Hussain, T. C. Dörge and T. J. Sørensen, *ACS Sens.*, 2019, **4**, 26–31.
- 4 J. Zhou, Y. Ren, Y. Nie, C. Jin, J. Park and J. X. J. Zhang, *Nanoscale Adv*, 2023, **5**, 2180–2189.
- 5 J.-T. Hou, W. X. Ren, K. Li, J. Seo, A. Sharma, X.-Q. Yu and J. S. Kim, *Chem. Soc. Rev.*, 2017, **46**, 2076–2090.
- 6 Y. Chen, C. Zhu, J. Cen, Y. Bai, W. He and Z. Guo, *Chem. Sci.*, 2015, **6**, 3187–3194.
- 7 P. Bhuinya, S. Guha, S. Roy, P. Dutta, S. K. Dey, P. K. Sukul, G. Das, T. Goswami and C. Kar, *ChemistrySelect*, 2024, **9**, e202403990.
- 8 N. Saleh, Y. A. Al-Soud and W. M. Nau, *Spectrochim. Acta. A. Mol. Biomol. Spectrosc.*, 2008, **71**, 818–822.
- 9 M. Matsui, T. Yamamoto, K. Kakitani, S. Biradar, Y. Kubota and K. Funabiki, *Dyes Pigments*, 2017, **139**, 533–540.
- 10 M. Baruah, W. Qin, N. Basarić, W. M. De Borggraeve and N. Boens, *J. Org. Chem.*, 2005, **70**, 4152–4157.
- 11 D. Jin, B. Wang, Y. Hou, Y. Du, X. Li and L. Chen, *Dyes Pigments*, 2019, **170**, 107612.
- 12 S. Ulrich, A. Osypova, G. Panzarasa, R. M. Rossi, N. Bruns and L. F. Boesel, *Macromol. Rapid Commun.*, 2019, **40**, 1900360.
- 13 C. Totland, P. J. Thomas, B. Holst, N. Akhtar, J. Hovdenes and T. Skodvin, *J. Fluoresc.*, 2020, **30**, 901–906.
- 14 F. Le Guern, V. Mussard, A. Gaucher, M. Rottman and D. Prim, *Int. J. Mol. Sci.*, 2020, **21**, 9217.
- 15 B. Gauthier-Manuel, C. Benmouhoub and B. Wacogne, *Sensors*, 2024, **24**, 1705.
- 16 Y. J. Kim, M. Jang, J. Roh, Y. J. Lee, H. J. Moon, J. Byun, J. Wi, S.-K. Ko and J. Tae, *Int. J. Mol. Sci.*, 2023, **24**, 15073.
- 17 P. Bhuinya, S. Guha, S. Roy, P. Dutta, S. K. Dey, P. K. Sukul, G. Das, T. Goswami and C. Kar, *ChemistrySelect*, 2024, **9**, e202403990.
- 18 K. Wang, Y.-L. Zhu, T.-F. Zheng, X. Xie, J.-L. Chen, Y.-Q. Wu, S.-J. Liu and H.-R. Wen, *Anal. Chem.*, 2023, **95**, 4992–4999.
- 19 W. Liu, X. Tian, S. Gong, Z. Meng, Y. Liang, Z. Wang and S. Wang, *J. Mol. Struct.*, 2024, **1299**, 137141.
- 20 S. Achelle, J. Rodríguez-López and F. Robin-le Guen, *J. Org. Chem.*, 2014, **79**, 7564–7571.
- 21 Z. Wang, H. Li, Z. Peng, Z. Wang, Y. Wang and P. Lu, *RSC Adv.*, 2020, **10**, 30297–30303.
- 22 X. Tang, Z. Zhu, Z. Wang, Y. Tang, L. Wang and L. Liu, *Spectrochim. Acta. A. Mol. Biomol. Spectrosc.*, 2020, **228**, 117845.
- 23 M.-S. Zhu, G. Zhang, Y.-J. Xu, R. Sun and J.-F. Ge, *Org. Biomol. Chem.*, 2023, **21**, 1992–2000.
- 24 S. Y. Bong, Z. Song, K. Kaur, N. Singh, Y. Park, J. Park and D. O. Jang, *Spectrochim. Acta. A. Mol. Biomol. Spectrosc.*, 2024, **323**, 124925.
- 25 A. E. Kopotilova, T. N. Moshkina, E. V. Nosova, G. N. Lipunova, E. S. Starnovskaya, D. S. Kopchuk, G. A. Kim, V. S. Gaviko, P. A. Slepukhin and V. N. Charushin, *Molecules*, 2023, **28**, 1937.
- 26 Z.-S. Huang, W. Zhang, M. Liang, S. Wang, Z. Zhang, Y. Jiang, X. Ye, L. Xie and Y.-Y. Quan, *Anal. Chim. Acta*, 2024, **1299**, 342434.
- 27 L.-X. Wang, Z.-H. Wang, X.-L. Sun, C.-T. Zi, X.-J. Wang and J. Sheng, *Bioorganic Chem.*, 2022, **121**, 105585.
- 28 Z. Xing, W. Wu, Y. Miao, Y. Tang, Y. Zhou, L. Zheng, Y. Fu, Z. Song and Y. Peng, *Org. Chem. Front.*, 2021, **8**, 1867–1889.
- 29 S. S. Roja, P. Sneha Sunil, M. M. Darussalam, V. Manoharan, J. Prakash and R. Ranjith Kumar, *Spectrochim. Acta. A. Mol. Biomol. Spectrosc.*, 2025, **333**, 125853.
- 30 Y. Kumar, N. Kumar Singh, S. Mukhopadhyay and D. Shankar Pandey, *Inorganica Chim. Acta*, 2023, **546**, 121294.
- 31 Y. Suzuki, J. Sawada, P. Hibner, H. Ishii, K. Matsuno, M. Sato, B. Witulski and A. Asai, *Dyes Pigments*, 2017, **145**, 233–238.
- 32 M. Motoyama, T. Doan, P. Hibner-Kulicka, R. Otake, M. Lukarska, J. Lohier, K. Ozawa, S. Nanbu, C. Alayrac, Y. Suzuki and B. Witulski, *Chem.-Asian J.*, 2021, **16**, 2087–2099.
- 33 K. Aoki, R. Osako, J. Deng, T. Hayashita, T. Hashimoto and Y. Suzuki, *RSC Adv.*, 2020, **10**, 15299–15306.

